Materials Today: Proceedings 49 (2022) 2761–2764

Contents lists available at ScienceDirect

Materials Today: Proceedings

journal homepage: www.elsevier.com/locate/matpr

Electronic transport of $ZnSnSb_2$ for thermoelectric application

Veera Prabu Kannan [a], Immanuel Paulraj [b], Vinothkumar Lourdhusamy [b], Chia-Jyi Liu [b,*], Sridharan Madanagurusamy [a,*]

[a] Functional Nanomaterials & Devices Lab, School of Electrical & Electronics Engineering, SASTRA Deemed to be University, Thanjavur 613 401, India
[b] Department of Physics, National Changhua University of Education, Changhua, Taiwan

ARTICLE INFO

Article history:
Available online 20 October 2021

Keywords:
$ZnSnSb_2$
Chalcopyrite
Thermoelectric
Low resistivity
Solid state reaction

ABSTRACT

Thermoelectric (TE) devices convert heat energy directly into electricity, which requires highly efficient, eco-friendly, and reliable materials. The chalcopyrite compound zinc tin antimonide ($ZnSnSb_2$) is a promising thermoelectric material that has high electrical conductivity, non-toxic, low cost, and plenty in nature. The $ZnSnSb_2$was synthesized by simple one-step Solid-State Reaction (SSR) and studied their microstructural and electronic transport properties. The X-Ray Diffraction (XRD) pattern of the $ZnSnSb_2$ exhibited a tetragonal crystal structure with $\frac{c}{a}$ ratio of 2 that indicates the valance band was degenerate, which was the reason for the low electrical resistivity of $ZnSnSb_2$ (0.32 mΩ-cm at 325 K). Furthermore, the thermopower exhibited p-type behaviour and the maximum power factor $ZnSnSb_2$ was found 39 μW/m-K^2 at 542 K.

Selection and peer-review under responsibility of the scientific committee of the Indo-UK International Virtual Conference on Advanced Nanomaterials for Energy and Environmental Applications (ICANEE-2020).

1. Introduction

TE devices are working under the principle of the Seebeck effect, which converts heat flux directly into electricity [1]. Thermoelectric devices are noise-free, high life span, eco-friendly, etc. The heat conversion efficiency of the thermoelectric materials calculated from the dimensionless figure of merit $zT = S^2T/\rho\kappa$, where ρ is electrical resistivity; S- is the thermopower; T is the absolute temperature and κ is total thermal conductivity, which can be written as $\kappa = \kappa_L + \kappa_e$ [2], where $\kappa_L$andκ_e are the lattice and electronic thermal conductivities respectively. The good TE material exhibits high power factor ($P.F = \sigma S^2$) and low κ_L. The Wiedemann-Frantz law gives the relation between the σ and κ_e, which is $\kappa_e = L\sigma T$, where L-is the Lorentz number. Telluride (Bi_2Te_3, PbTe), zintl (Mg_3Sb_2, Mg_3Bi_2), oxide (In_2SnO_3, TiO_2) metal Chalcogenides (CuS, SnSe) based materials are mostly used for TE application [3–8]. For the commercialization of thermoelectric material, $zT \approx 1$ is considered as standard [9]. However, their commercialization is restricted by toxic, expensive materials, and low efficiency [10]. Chalcopyrite is a promising material for TE application due to its high electrical conductivity and low k_L. Tellurium-based chalcopyrite materials such as $CuGaTe_2$, $AgGaTe_2$, and $CuInTe_2$ show high P.F and low k_L. Ken Kurosaki et al. [11]reported the $CuGaTe_2$ has the highest power factor of 13.5 μW/cmK^2 and the corresponding and zT is 1.4 at 950 K. Ruiheng Liu et al. [12]reported p-type $CuInTe_2$, it has a high zT value of 1.18 at 850 K. Aikebaier Yusufu et al. [13] reported that the reduction of Ag (x = 0, 0.01, 0.03, 0.05, and 0.07) simultaneously decrease the resistivity and thermopower in $Ag_{1-x}GaTe_2$ (x = 0.05) and showed a high zT of 0.77 at 850 K with the maximum P.F of 3.3 μW/cmK^2 at 700 K. Moreover the Ag lattice defect increase the phonon scattering leads the reduction of k_L. However, these Chalcopyrite materials contain scarce, more expensive and toxic elements; $ZnSnSb_2$ is the promising material for TE application with eco-friendly, non-toxic, inexpensive, and abundant in nature [9]. It has expected that the $ZnSnSb_2$ has high electrical conductivity due to the tetragonal crystal structure with c/a = 2 increases the symmetry of the crystal that leads to band convergence [14], and also we expect low lattice thermal conductivity due to the presence of heavy elements such as Sn and Sb [15]. This work investigated the electronic transport properties, namely, electrical resistivity, thermopower (S), and power factor ($S^2\sigma$) of $ZnSnSb_2$.

* Corresponding authors.
E-mail addresses: liucj@cc.ncue.edu.tw (C.-J. Liu), m.sridharan@ece.sastra.edu (S. Madanagurusamy).

https://doi.org/10.1016/j.matpr.2021.09.301
2214-7853/
Selection and peer-review under responsibility of the scientific committee of the Indo-UK International Virtual Conference on Advanced Nanomaterials for Energy and Environmental Applications (ICANEE-2020).

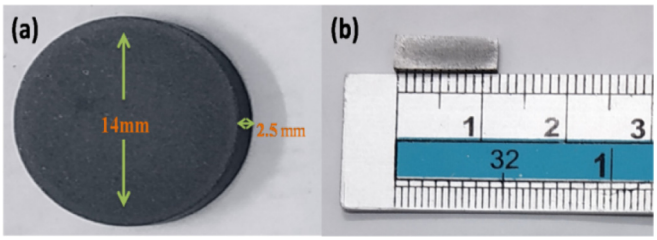

Fig. 1. (a) Sintered; (b) cut and polished pellet of $ZnSnSb_2$.

2. Materials and methods

2.1. Preparation of $ZnSnSb_2$

The measured starting materials: Zinc (Zn, Purity 99.9%), Tin (Sn, Purity 99.80%), and Antimony (Sb, Purity 99.5%) were mixed and ground homogeneously and subjected to cold-pressed by applying 63 MPa of pressure. The resulting pellet (2.5 mm thick × 14 mm in diameter) was transferred to a 16 mm diameter Pyrex tube, which was evacuated by rotary and diffusion pump to $\acute{3} \times 10^{-5}$ Torr and then sealed. The sealed Pyrex tube was transferred into the box furnace, heated up to 853 K for 6 h, and cooled down to room temperature naturally. The obtained ingot was crushed and ground manually for further use, cold-pressed into a pellet at 159 MPa. The resulting pellet was evacuated and sealed using a rotary and diffusion pump. The sealed Pyrex tube was sintered at 573 K for 6 h and naturally cooled down to room temperature. To study the TE properties of the pellet, which was cut and polished by diamond saw cutter and sandpaper, respectively.

2.2. Sample characterization

The powder XRD patterns of prepared materials were obtained using the Shimadzu diffractometer – 6000 (with Fe K_α target) from 10° to 90° in steps of 0.02°. Temperature dependence electrical resistivity and thermopower were measured by Setsram SeebeckPro systems simultaneously between 325 and 550 K in steps of 25 K. The electrical resistivity and thermopower error is about ±10 and ±7%, respectively. The pellet was cut and polished into the suitable dimension of length × breath × width 11 mm × 2 mm × 2 mm for TE measurement. Fig. 1 shows the image of (a). sintered and (b). cut and polished pellet.

3. Results and discussion

The $ZnSnSb_2$ was synthesized using a simple one-step SSR method and evaluated its TE properties from 300 to 550 K. Fig. 2 (a). shows the XRD pattern all the peaks 30.82, 36.51, 51.57, 61.38, 76.01, and 84,30 matches with the JCPDS card no 00–051-0882 and the corresponding planes are (112), (200), (204), (312), (400) and (316) respectively, confirmed the tetragonal crystal structure of chalcopyrite $ZnSnSb_2$ with the space group of I-42d (122). The low intense peak arises due to the presence of SnSb and ZnSb [15]. The lattice constant of the tetragonal $ZnSnSb_2$ were calculated a = b = 6.277 Å, c = 12.554 Å and c/a ratio is 2.0 and are well-matched with the reported values [9]. From Debye-Scherer's formula, ($D = k\lambda / \beta \cos\theta$) the crystallite size was calculated was 73.14 nm.

The temperature dependence of the ρ,*S* and power factor ($P.F = \frac{S^2}{\rho}$) of the sample $ZnSnSb_2$ are summarized in Fig. 3. As shown in Fig. 3(a), the ρ of the sample increased with increasing temperature, indicating the semi metallic or degenerate semiconductor behaviour [15].

The ρ values are very small, which is less than 0.5 mΩ-cm. Between 300 and 550 K; the electrical resistivity varies little with temperature from 0.32 to 0.41 mΩ-cm, respectively. The comparison of synthesis method and electrical resistivity of tetragonal chalcopyrites are presented in Table 1. The thermopower showed in Fig. 3(b), the value is positive, which indicates that most charge carriers are holes in ZnSnSb2 and reveal the P-type conduction. The magnitude is increased with an increase in temperature. The temperature dependence thermopower increased significantly and correlated with Mott's equation. The thermopower of degenerate semiconductors writes using Motts Eq. (1) [16]

$$S = \frac{\pi^2 K_B^2 T}{3q} \frac{d \ln \sigma(E)}{dE} | E = E_F \propto - \frac{T}{N_{tot}(E)} \frac{dN_{tot}(E)}{dE} | E = E_F \quad (1)$$

where K_B is the Boltzmann constant, q is the elementary electric charge, σ (E) is the electrical conductivity and $N_{tot}(E)$ is the value of density of states (DOS), respectively. From *S* and ρ the calculated power factor (P.F) showed in Fig. 3(c). The calculated P.F of the prepared $ZnSnSb_2$ increases with function temperature. The $ZnSnSb_2$

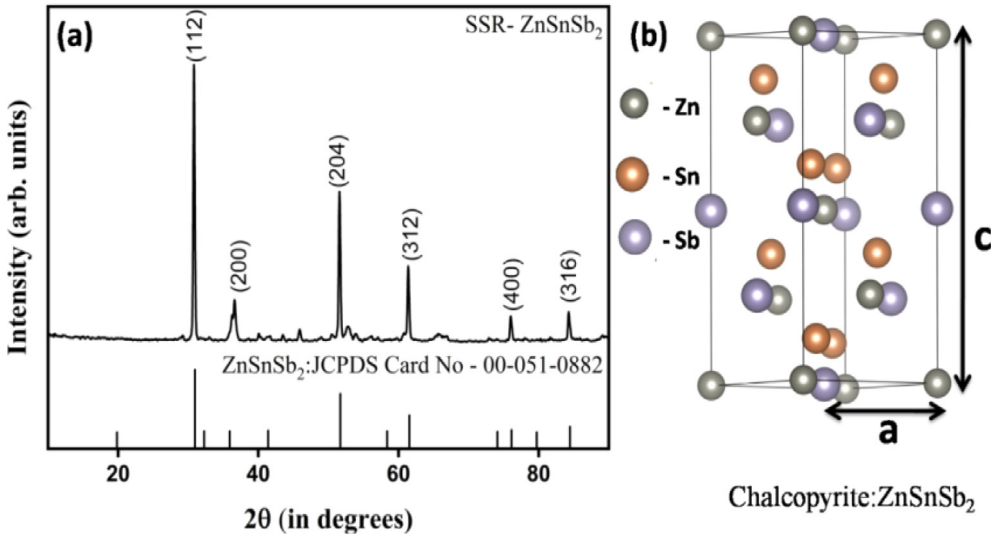

Fig. 2. (a) XRD pattern of $ZnSnSb_2$ and (b) Tetragonal Chalcopyrite crystal structure.

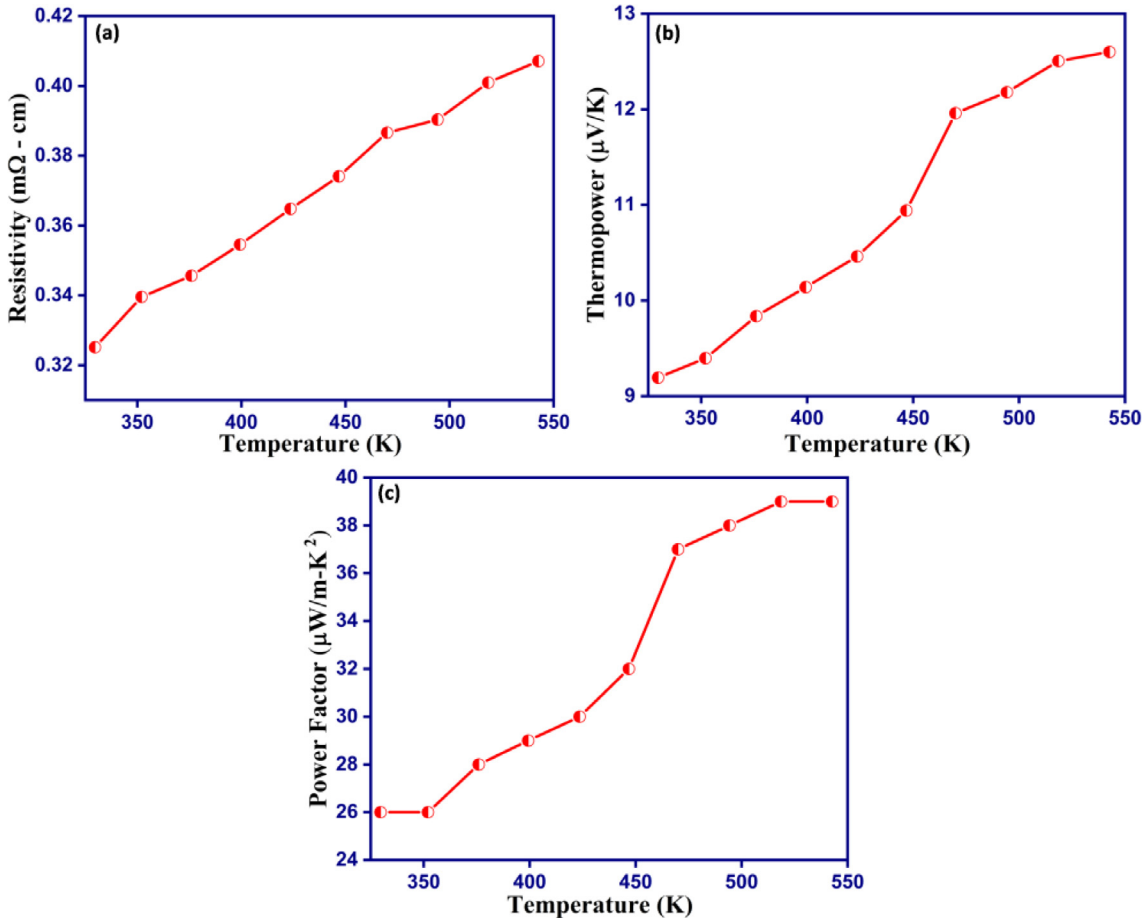

Fig. 3. Temperature dependence electric transport properties of $ZnSnSb_2$; (a) electrical resistivity, (b) thermopower and (c) Power factor.

Table 1
Comparison synthesize method and electrical resistivity of tetragonal Chalcopyrites.

Materials	Synthesize Method	Electrical Resistivity	Ref.
$CuInTe_2$	Vacuum melting at 1173 K for 10 h and Spark Plasma Sintering (SPS) at 873 K for 5–10 mins	6.9 mΩ-cm @ 300 K	[12]
$CuGaTe_2$	Vacuum melting at 1173 K for 12 h and annealed at 773 K for 3 days, hot pressing at 873 K for 3 h	4.41 mΩ-cm @ 950 K	[11]
$AgGaTe_2$	Vacuum melting at 1273 K for 24 h and hot pressing at 773 K for 2 h	~80 mΩ-cm@ 750 K	[13]
$ZnSnSb_2$	Vacuum melting at 923 K for 12 h	0.3 mΩ-cm @ 300 K	[15]
$ZnSnSb_2$	Vacuum melting at 923 K for 12 h and annealed at 533 K for 24 h, SPS at 453for 15 mins	~0.6 mΩ-cm@ 300 K	[9]
$ZnSnSb_2$	Vacuum melting at 853 K for 6 h and sintered at 573 K for 6 h	0.32 mΩ-cm @ 325 K	Present work

exhibited the maximum power factor of 39 μW/m-K^2 at 542 K. From the results, the $ZnSnSb_2$ exhibits low thermopower and P.F values, so the $ZnSnSb_2$ is the poor TE material for the power generation application. The ρ is ultralow at room temperature, so further optimization in the composition and thermopower is needed for power generation application.

4. Conclusion

The $ZnSnSb_2$ was synthesized by a simple one-step SSR method; $ZnSnSb_2$ exhibits the tetragonal structure. From the temperature-dependent electrical studies, the ZnsnSb2 shows the ultra-low resistivity of 0.32 mΩ-cm at 325 K. The resistivity is less than 0.5 mΩ-cm throughout the whole temperature range. The maximum power factor of 39 μW/m-K^2 was observed at 542 K. However, the thermopower and power factor are pretty low. Further optimization is required to improve the thermopower and power factor of $ZnSnSb_2$ for power generation application.

Declaration of Competing Interest

The authors declare that they have no known competing financial interests or personal relationships that could have appeared to influence the work reported in this paper.

Acknowledgements

The authors MS & KVP thank SASTRA Deemed to be University, Thanjavur, for extending infrastructure support to carry out this work. In addition, the authors MS & KVP wish to express their sincere thank to National Changhua University of Education (NCUE), Taiwan for various characterization facilities. KVP expresses thanks to the University Grants Committee (UGC) for awarding a

Junior Research Fellowship under the Maulana Azad National Fellowship (MANF) scheme [Ref.: MANF-2018-19-TAM-98930 dated 14.08.2019]. This work was supported by Ministry of Science and Technology of Taiwan under the TEEP internship programme (Grant No.107-2112-M-018-006-MY3).

References

[1] M. Hamid Elsheikh, D.A. Shnawah, M.F.M. Sabri, S.B.M. Said, M. Haji Hassan, M. B. Ali Bashir, M. Mohamad, A review on thermoelectric renewable energy: Principle parameters that affect their performance, Renew. Sustain. Energy Rev. 30 (2014) 337–355, https://doi.org/10.1016/j.rser.2013.10.027.

[2] K.-C. Chang, C.-J. Liu, An algorithm of calculating transport parameters of thermoelectric materials using single band model with optimized integration methods, Comput. Phys. Commun. 247 (2020) 106875, https://doi.org/10.1016/j.cpc.2019.106875.

[3] M. Calderón-Cueva, W. Peng, S.M. Clarke, J. Ding, B.L. Brugman, G. Levental, A. Balodhi, M. Rylko, O. Delaire, J.P.S. Walsh, S.M. Dorfman, A. Zevalkink, Anisotropic Structural Collapse of Mg3Sb2and Mg3Bi2at High Pressure, Chem. Mater. 33 (2) (2021) 567–573, https://doi.org/10.1021/acs.chemmater.0c03678.

[4] B. Arjunkumar, G. Ramalingam, M. Ramesh, J.S. Ponraj, K.V. Rao, Investigation of uni-directional nanorods composed microspheres and branched TiO2 nanorods towards solar cell application, Mater. Lett. 273 (2020) 127900, https://doi.org/10.1016/j.matlet.2020.127900.

[5] R. Perumalsamy, K. Kaviyarasu, S. Nivetha, A. Ayeshamariam, N. Punithavelan, D. Letsholathebe, G. Ramalingam, M. Jayachandran, Preparation, Characterization and Structure Prediction of In 2 SnO 3 and Spectroscopic (FT-IR, FT-Raman, NMR and UV-Visible) Study Using Computational Approach, J. Nanosci. Nanotechnol. 19 (6) (2019) 3511–3518, https://doi.org/10.1166/jnn.2019.16097.

[6] G. Ramalingam, R. Vignesh, C. Ragupathi, C.M. Magdalane, K. Kaviyarasu, J. Kennedy, Electrical and chemical stability of CuS nanofluids for conductivity of water soluble based nanocomposites, Surf. Interfaces 19 (2020) 100475, https://doi.org/10.1016/j.surfin.2020.100475.

[7] Z.-R. Yang, W.-H. Chen, C.-J. Liu, Synthesis and electronic transport of hydrothermally synthesized p-type Na-doped SnSe, J. Electron. Mater. 46 (5) (2017) 2964–2968, https://doi.org/10.1007/s11664-016-5084-2.

[8] F.-H. Lin, C.-J. Liu, A simple energy-saving aqueous synthesis of Bi 2 Te 3 nanocomposites yielding relatively high thermoelectric power factors, Ceram. Int. 45 (7) (2019) 9397–9400, https://doi.org/10.1016/j.ceramint.2018.08.170.

[9] A. Nomura, S. Choi, M. Ishimaru, A. Kosuga, T. Chasapis, S. Ohno, G.J. Snyder, Y. Ohishi, H. Muta, S. Yamanaka, K. Kurosaki, Chalcopyrite ZnSnSb 2: A Promising Thermoelectric Material, ACS Appl. Mater. Interfaces 10 (2018) 43682–43690, https://doi.org/10.1021/acsami.8b16717.

[10] J. Zhang, L. Song, S.H. Pedersen, H. Yin, L.T. Hung, B.B. Iversen, Discovery of high-performance low-cost n-type Mg3Sb2-based thermoelectric materials with multi-valley conduction bands, Nat. Commun. 8 (2017) 1–8, https://doi.org/10.1038/ncomms13901.

[11] T. Plirdpring, K. Kurosaki, A. Kosuga, T. Day, S. Firdosy, V. Ravi, G.J. Snyder, A. Harnwunggmoung, T. Sugahara, Y. Ohishi, H. Muta, S. Yamanaka, Chalcopyrite CuGaTe 2: A high-efficiency bulk thermoelectric material, Adv. Mater. 24 (27) (2012) 3622–3626, https://doi.org/10.1002/adma.v24.2710.1002/adma.201200732.

[12] R. Liu, L. Xi, H. Liu, X. Shi, R. Liu, L. Chen, Ternary compound CuInTe2: A promising thermoelectric material with diamond-like structure, Chem. Commun. 48 (2012) 3818–3820, https://doi.org/10.1039/c2cc30318c.

[13] A. Yusufu, K. Kurosaki, A. Kosuga, T. Sugahara, Y. Ohishi, H. Muta, S. Yamanaka, Thermoelectric properties of Ag 1-xGaTe 2 with chalcopyrite structure, Appl. Phys. Lett. 99 (2011) 8–11, https://doi.org/10.1063/1.3617458.

[14] W.G. Zeier, H. Zhu, Z.M. Gibbs, G. Ceder, W. Tremel, G.J. Snyder, Band convergence in the non-cubic chalcopyrite compounds Cu2MGeSe4, J. Mater. Chem. C. 2 (47) (2014) 10189–10194, https://doi.org/10.1039/C4TC02218A.

[15] A. Tengå, F. Javier García-García, A.S. Mikhaylushkin, B. Espinosa-Arronte, M. Andersson, U. Häussermann, Sphalerite – Chalcopyrite polymorphism in semimetallic ZnSnSb, Chem. Mater. 17 (2005) 6080–6085, https://doi.org/10.1021/cm0516053.

[16] M. Ito, Y. Ohishi, H. Muta, K. Kurosaki, S. Yamanaka, Thermoelectric properties of Zn-Sn-Sb based alloys, Mater. Res. Soc. Symp. Proc. 1314 (2011) 70–75, https://doi.org/10.1557/opl.2011.618.